AGU ADVANCING EARTH AND SPACE SCIENCE

Geophysical Research Letters®

RESEARCH LETTER
10.1029/2021GL097223

A Novel Framework for Simulating Particle Deposition With Moving Bedforms

Yoni Teitelbaum[1], Tomer Shimony[1], Edwin Saavedra Cifuentes[2], Jonathan Dallmann[3,4], Colin B. Phillips[5], Aaron I. Packman[2], Scott K. Hansen[1], and Shai Arnon[1]

[1]Zuckerberg Institute for Water Research, The Jacob Blaustein Institutes for Desert Research, Ben-Gurion University of the Negev, Beersheba, Israel, [2]Civil and Environmental Engineering, Northwestern University, Evanston, IL, USA, [3]Mechanical Engineering, Northwestern University, Evanston, IL, USA, [4]Center for Preparatory Studies, Nazarbayev University, Astana, Kazakhstan, [5]Civil and Environmental Engineering, Utah State University, Logan, UT, USA

Key Points:

- A moving-interface model for particle deposition in streambeds under moving bedform conditions is introduced
- Model reproduces experimental observations of the formation of a clay layer below the bedform scour zone
- Bedform celerity and particle filtration have interacting effects on the rate and location of particle deposition

Supporting Information:

Supporting Information may be found in the online version of this article.

Correspondence to:

Y. Teitelbaum,
teitelba@post.bgu.ac.il

Citation:

Teitelbaum, Y., Shimony, T., Saavedra Cifuentes, E., Dallmann, J., Phillips, C. B., Packman, A. I., et al. (2022). A novel framework for simulating particle deposition with moving bedforms. *Geophysical Research Letters*, *49*, e2021GL097223. https://doi.org/10.1029/2021GL097223

Received 25 NOV 2021
Accepted 31 JAN 2022

Abstract Previous modeling studies of hyporheic exchange induced by moving bedforms have used a moving reference frame, typically corresponding to an individual moving bedform. However, this approach is not suitable for simulating the exchange and accumulation of immobile fine particles beneath moving bedforms, which commonly occurs in sand-bed streams, as both moving and stationary features must be considered. Here we present a novel simulation framework that may represent arbitrarily shaped, generally aperiodic mobile bedforms within a stationary reference frame. We combine this approach with particle tracking to successfully reproduce observations of clay deposition in sand beds, and the resulting development of a low-conductivity layer near the scour zone. We find that increased bedform celerity and filtration both lead to a shallower depth of clay deposition and a more compact deposition layer. While increased filtration causes more clay to deposit, increased celerity reduces deposition by flattening hyporheic exchange flowpaths.

Plain Language Summary Stream water flows into and out of sand ripples along the stream bed. It is also common for streambed sand ripples to migrate downstream due to erosion and deposition of sediment. Mathematical models that simulate the flow of stream water into and out of streambed ripples have typically done so from the perspective of a viewer who moves downstream with the ripple. This approach can be useful but is less suitable for representing the accumulation of material deposited by the water flowing through the ripple. We present a novel mathematical model that represents moving sand ripples from the perspective of a viewer who is standing still and watching the ripples go by. Simulation results successfully reproduce experimental observations of the accumulation of material deposited by water flowing through the ripple. Ripples that move faster deposit material at shallower depths and deposit less of the material that flows through the ripple. Deposited particles with a higher tendency to become trapped between streambed sand grains will also deposit at shallower depths. This model will provide new insights into the transport and deposition of contaminants that enter streams and rivers.

1. Introduction

Fine suspended particles are ubiquitous in streams and rivers. Suspended material typically includes sedimentary particles (Wharton et al., 2017), particulate organic matter (Johnson et al., 2018), microplastics (Li et al., 2020), and microbiota such as bacteria, algae, and viruses (Lenaker et al., 2018). Transport and deposition of fine suspended particles play a key role in regulating river-groundwater interactions, river morphodynamics, and hyporheic biogeochemistry (Boano et al., 2014). Clay particle deposition decreases streambed hydraulic conductivity by filling porespace, ultimately clogging the bed, altering patterns of porewater flow, and degrading the benthic and hyporheic ecosystem (Brunke, 1999; Brunke & Gonser, 1997; Fox et al., 2018). Clay in the streambed can also reduce bed sediment motion (Dallmann et al., 2020). The deposition of fine particulate organic matter drives hyporheic metabolism (Newbold et al., 2005) and plays an important role in fluvial carbon cycling (Brunke & Gonser, 1997; Hope et al., 1994). Additionally, fine sediment particles play an important role in the colloid-facilitated transport of sorbed metals (Droppo et al., 2014; Foster & Charlesworth, 1996), as well as the accumulation of contaminants in bed sediment (Arce et al., 2017; Stone & Droppo, 1994). Despite the importance of spatial patterns of particle deposition for hyporheic ecosystems, fluvial biogeochemical processes, and river contamination most studies of riverine fine particles focus on the water column (Drummond et al., 2019; Park & Hunt, 2018; Wolke et al., 2020). Considerably less effort has been put into understanding the dynamics

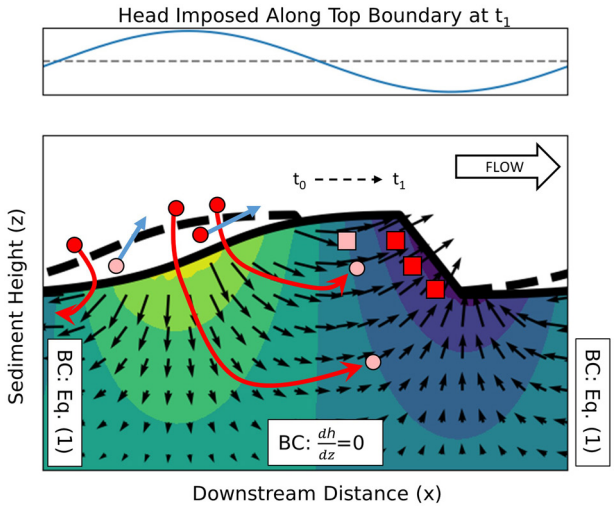

Figure 1. Schematic diagram of moving-boundary model for fine particle transport and deposition. The model represents the passage of a series of bedforms, but only a single bedform is illustrated here for simplicity. The dashed line shows the shape of the domain top boundary (sediment-water interface) at time t_0, while the solid line shows the boundary shape after migration at t_1. Head within the bed at t_1 is shown by the colored contours; bright colors are high-pressure areas, while dark colors show low-pressure areas. Black arrows show instantaneous hyporheic streamlines that result from the head gradients within the bed at t_1. Circles and squares indicate particles that enter the bed via pumping (at the upstream face of the bedform) and turnover (at the downstream face of the bedform), respectively. Particles with a red interior are mobile in the streamwater and hyporheic porewater, while particles with a pink interior have been deposited. Red lines illustrate example flow paths followed by particles. Particle remobilization from the bed by scouring between t_0 and t_1 is represented by blue arrows.

of fine particle transport within the bed and the resulting spatial patterns of particle accumulation (e.g., Drummond et al., 2017; Harvey et al., 2012; Phillips et al., 2019).

A principal mechanism of fine suspended particle delivery into streambeds is hyporheic exchange flux (HEF), particularly advective HEF induced by stream bedforms (Packman & Mackay, 2003; Partington et al., 2017). Particle deposition in streambeds due to HEF induced by stationary bedforms has been observed in both flume experiments (Fox et al., 2018; Jin et al., 2019; Packman et al., 2000b; Rehg et al., 2005) and simulated using numerical models (Packman et al., 2000a; Preziosi-Ribero et al., 2020). However, many natural sand-bed streams have continuous bed sediment transport (Einstein, 1950; Engelund & Hansen, 1967). Bed sediment is eroded from the upstream (stoss) side of the bedform and redeposited on the downstream (lee) side, causing the bedforms to migrate downstream. During bedform movement fine particles and pore water are released from the stoss side of the bedform by erosion, while surface water and suspended fine particles become trapped by lee-side re-deposition of bed sediment (Packman & Brooks, 2001). Hyporheic exchange due to the aforementioned mechanism is referred to as "turnover" (Elliott & Brooks, 1997).

Previous analyses of HEF under moving bedforms have employed a Lagrangian frame of reference that travels downstream with the bedform, starting with Elliott & Brooks (1997) for solutes. In recent work, the Lagrangian reference frame has been adopted by several researchers to study oxygen consumption and nutrient transformation in the hyporheic zone (Kessler et al., 2015; Zheng et al., 2019) and marine sediments (Ahmerkamp et al., 2015). This approach is adequate for analyses of the fate of mobile species but is less suitable for tracking the accumulation of immobilized particles at a given location over arbitrary lengths of time.

Here we present a model that combines four key features needed to capture the spatiotemporal dynamics of fine particle deposition under moving bedforms: realistic bedform shape, the passage of a series of bedforms through a fixed frame of reference, hyporheic particle transport and deposition, and long-term particle accumulation that produces spatial patterns in the bed. We then use this model to explain coupled clay-sand dynamics that control short-term particle transport and, over longer timescales, yield depositional patterns commonly found in rivers.

2. Methods

We implemented a 2D model of particle deposition with moving bedforms in Python (Harris et al., 2020; Hunter, 2007; McKinney, 2010; Virtanen et al., 2020), with the bed surface specified analytically using mathematical functions in order to discretize natural bedform geometries. The modeling framework and processes captured by the model are illustrated in Figure 1. We use a Bezier curve to define the upstream face of the bedform and a linear function to define the downstream face (Text S1 in Supporting Information S1). Since a Bezier curve is a polynomial defined based on user-specified control points, this choice provides an intuitive way to represent arbitrary bedform shapes. The two-part function delineates the top boundary of the domain, which represents the sediment-water interface. At each timestep, the top boundary shape changes as bedforms are migrated downstream at a constant celerity.

Head is imposed along the top boundary of the domain using a sinusoidal head function (Elliott & Brooks, 1997; Text S2). A no-flux boundary condition is imposed along the bottom of the domain. At the left and right boundaries of the domain, the head at the surface is attenuated toward zero with increasing depth using an exponential decay function (Elliott & Brooks, 1997):

$$h(z) = h(z_0) \cdot exp(-rd) \quad (1)$$

where $h(z)$ is head at bed height with vertical coordinate z measured upward from the base of the bed, z_0 is the height of the top of the bed, r is the decay rate $2\pi/\lambda$, and $d = (z_0 - z)$ is the depth of z below the bed surface. Previous works have all utilized periodic boundary conditions along the side boundary, an unduly restrictive choice because the shape of hyporheic flow paths is dictated by the shape of the bed surface, which is typically not periodic in sand-bed rivers (McElroy & Mohrig, 2009). Exponentially attenuating the head along the side boundary removes the reliance on this assumption, as it relies only on the imposed head at the top of the side boundary without making assertions about any other point in the domain.

At each timestep, the model is treated as being at a steady state. The instantaneous system geometry is treated as fixed at each timestep, and the effects of sand and water compressibility are assumed to be negligible at the scale addressed by this model. Thus, at each timestep, the instantaneous head field in the bed is computed based on the bed surface geometry using the Laplace equation, which describes steady-state groundwater flow (Elliott & Brooks, 1997; Zheng et al., 2019):

$$\nabla^2 h = 0 \tag{2}$$

where h is hydraulic head (cm). This equation is solved using a 2D finite-difference scheme over the domain grid (Text S1 in Supporting Information S1). Streamlines in the bed are then computed using Darcy's law.

Porewater flow, solute transport, particle transport, and deposition within the bed are represented using a particle-tracking method. Fluid and suspended particles within the bed are propagated in each timestep in accordance with the instantaneous porewater velocity field obtained from the pseudo-steady velocity distributions. Particle deposition is represented using colloid filtration theory, following the earlier work of Packman et al. (2000a):

$$\frac{dC_m}{ds} = -\lambda_f C_m \tag{3}$$

where C_m is the suspended particle concentration, s is the distance traveled in the bed, and λ_f is the filtration coefficient. Consequently, the distance that an individual particle travels before depositing follows an exponential distribution:

$$D \sim Exp(s; \lambda_f) \tag{4}$$

where D is the distance traveled by the particle. The particle's probability of depositing at any location in the bed within a given timestep is given by the cumulative distribution function (CDF) of Equation 4:

$$F(s) = 1 - e^{-\lambda_f s} \tag{5}$$

In each timestep, each particle's displacement due to advection is computed. The advective displacement is then used to compute the particle's probability of depositing on that timestep using Equation 5. If the particle has not deposited during the current timestep, the particle is propagated by displacement due to both advection and dispersion. Longitudinal dispersivity α_L was set to 0.063 cm (Toride et al., 1995). Transverse dispersivity was set to $\alpha_T = 0.1\alpha_L$.

Once a particle has deposited, it is assumed not to remobilize except due to bedform scour. The average particle residence time in the bed is greater than the average time required for bedforms to travel one wavelength downstream. Thus, particle transport in the bed reflects the passage of multiple bedforms (and associated porewater flow), and the particle tracking model incorporates the full time-history of the bed profile and hyporheic flow field. The number and location of particles entering the bed due to pumping are calculated using the spatial distribution of HEF along the stoss side of the bedform (Text S1 in Supporting Information S1). The number of particles entering the lee face of the bedform is simulated using the incoming flux due to turnover, which is calculated by the following equation:

$$Q_t = c \cdot dt \cdot h_l \cdot w \cdot \theta \tag{6}$$

where Q_t is the flux (cm^3/s), c is the celerity (cm/s), dt (s) is the amount of time that passes per model timestep, h_l is the height of the lee face of the bedform, w is the width of the channel, and θ is the porosity of the sand. No particles are released within one bedform wavelength of the side boundaries in order to avoid any possible effects of the side boundary conditions (Text S2 in Supporting Information S1). The channel width w is included

to convert 2D flow paths computed by the model into volumetric flux across the sediment-water interface. We impose a constant concentration of particles in the water column, which does not change in response to particle exchange with the bed and deposition. This corresponds to the common case of large input of fine particles from upstream relative to the instantaneous exchange flux.

The modeled domain that we use in the simulations is 150 cm long. The bedforms are 25 cm long and 2.5 cm in height. The domain thus accommodates six bedforms (Text S2 in Supporting Information S1). The bed sediment below the bedforms is 20 cm thick, allowing domain height to vary from 20 to 22.5 cm. Channel width w is 30 cm to facilitate comparison with simulation results with the experimental observations of Teitelbaum et al. (2021). Stream water depth is 12 cm. The sand has a porosity of $\theta = 0.33$, hydraulic conductivity of 0.12 cm/s, and D_{50} of 0.31 mm. The sediment bed and its properties are assumed to be homogeneous and unchanging over time. Thus, for example, particle erosion, sorting, and compaction is not considered. The choice of the modeled physical conditions is based on typical characteristics of sand material, as used by Teitelbaum et al. (2021), to facilitate the comparison of simulation results with the experimental observations. Because we use a wider range of flow conditions in the simulations than appear in Teitelbaum et al. (2021), criteria for bedform formation and movement were implemented to ensure that the model is used under realistic conditions (Text S3 in Supporting Information S1, Data Set S1).

Simulations are run at filtration coefficients of 0.1 to 0.9/cm and bedform celerities of 0.6, 6, 30, 60, and 90 cm/hr. For each celerity, the corresponding streamwater velocity is calculated using the relationship from Snishchenko and Kopaliani (1978):

$$c = 0.019V \cdot Fr^{2.9} \tag{7}$$

where c is bedform celerity (m/s), V is the average streamwater velocity (m/s), Fr is the Froude number $(V/(gH)^{1/2})$, g is the gravitational constant and H is the water depth (m). We then use the physical parameters of the sand and the water to calculate a set of metrics to ensure that the criteria for bedform formation are fulfilled. Detailed calculations are represented in Text S3 in Supporting Information S1 and Data Set S1. The first criterion for bedform formation is that $Fr \leq Ft$ (Karim, 1995). If that condition holds, D^* and T^* are calculated to test whether and what type of bedforms will form (van Rijn, 1993). It is expected that ripples will form when $1 < D^* < 10$ and $0 < T^* < 10$. This implies that the bed will be stationary under a flow velocity of 0.1 m/s, while the rest of the flow conditions are expected to form ripples. Ripple wavelength and height depend on particle D_{50} (Lichtman et al., 2018; Raudkivi, 1997; Soulsby et al., 2012). Thus we used the same ripple geometry in all the simulations. Finally, the shear velocity, shear stress, and shields parameters are reported as parameters that control the movement of the bed.

3. Results and Discussion

Model validation occurred in two steps. Simulated HEF was compared to HEF measured during experiments under similar conditions (Fox et al., 2018; Teitelbaum et al., 2021) using linear regression. Simulated HEF was found to track well with experiments ($y = 1.18x$, $r^2 = 0.96$, Text S4 in Supporting Information S1). Simulated particle deposition profiles were also compared with the experimental observations of Teitelbaum et al. (2021) and found to be statistically equivalent (paired z-test, $z = -5.34 \times 10^{-16}$, $p > 0.05$; Text S5 in Supporting Information S1). Furthermore, simulated particle deposition profiles asymptotically converged to the pattern observed in experiments (Text S6 in Supporting Information S1). The deposition profile converges because of the passage of many bedforms: while there is a different pattern of HEF and particle transporting within each individual bedform, all bedforms contribute to the accumulation of particles below the scour zone.

Simulations reproduced experimental observations of both a conservative tracer and kaolinite deposition previously presented by Teitelbaum et al. (2021) (Figure 2). The distribution of the conservative tracer in the bed creates a conchoidally-shaped plume beneath each bedform (Figure 2b), as water and solutes enter the bed on the stoss side of the bedform (high pressure zone) and migrate along flow paths that eventually return to the stream at the low-pressure zones near the lee side of the bedform (see also Figure 1). This shape resembles the dye plumes that were observed during experiments (Figure 2c). The flow field imposed by the bedform migrates with the bedform as it moves downstream, so the solute plumes migrate with the bedforms as well (see Movie S1 and Teitelbaum et al. [2021]). The highest concentration of the dye in the bed occurred between the heights of

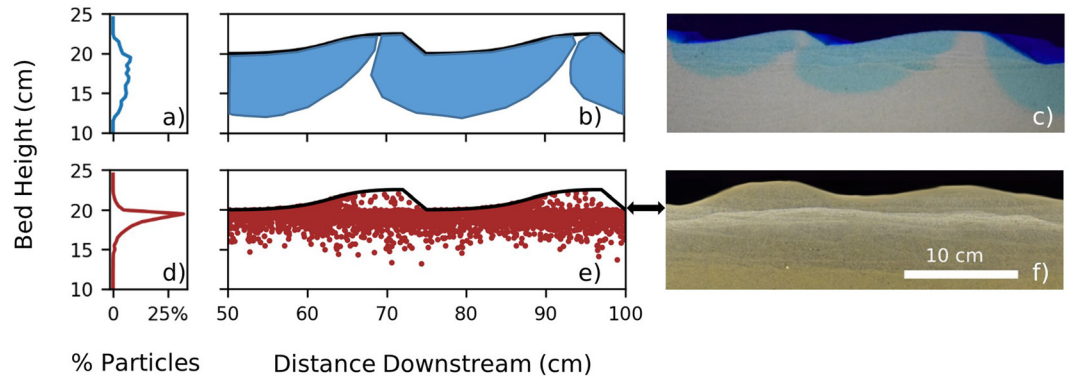

Figure 2. Comparison of particle transport simulations against experimental observations. The first row shows the distribution of the conservative tracer in (a) and (b) from the simulation while panel (c) shows a photograph of conservative dye plumes that were observed during tracer experiments in a flume. The second row shows the model results for deposited particles in (d) and (e) and a picture (f) from an experiment with kaolinite clay deposition under moving bedforms (Teitelbaum et al., 2021). Deposited clay is visible as a horizontal white layer just below the level of the troughs (f). The arrows between (e) and (f) represent the depth of the most frequent scour, below which most of the deposition occurs. The profiles in panels (a) and (d) show particle concentration by depth as a percentage of all particles shown in (b) and (e), respectively. Height is measured from the bottom of the model domain. The distance downstream shows the horizontal location within the modeling domain.

19.5–20 cm above the model bottom, that is, just below the line of most frequent scour depth (MFSD; Figure 2a). For the purposes of this calculation, the bed was divided into horizontal layers of 0.5 cm depth, and particle concentration versus depth was expressed as a percentage of particles in a given layer.

Particle deposition resulted in accumulation primarily within a layer just below the MFSD (Figures 2d–2f, Movie S2). This location was also where the maximum concentration of deposited particles was found (Figure 2d). This deposition pattern has also been observed in various flume experiments that used kaolinite clay particles (Dallmann et al., 2020; Packman & Brooks, 2001; Rehg et al., 2005; Teitelbaum et al., 2021), and field measurements (Harvey et al., 2012). Particle concentration decreased sharply with depth in the bed and the concentration dropped to zero within several cm (Figure 2d). Fewer particles are deposited at deeper locations than at shallower ones because particle concentration in porewater decreases exponentially with distance traveled in the bed due to filtration (Equation 3). At the end of each simulation, only a relatively small number of deposited particles could be found above the line of MFSD, that is, in the moving fraction of the bed. Particles that deposit there will necessarily be resuspended by erosion after spending some time in the bed (Figure 1, Movie S2). The vertical pattern of particle deposition is clear evidence of the averaging effect caused by the passage of many bedforms. This behavior has been observed previously (Dallmann et al., 2020; Teitelbaum et al., 2021), but our model is the first to show that downward particle fluxes underneath bedforms asymptotically yield a consistent depositional profile of fine particles below the scour zone.

After confirming that the model reproduces experimentally observed patterns, we assess how clay-sand interactions (i.e., filtration) and bedform celerity influence particle deposition. Increasing the filtration coefficient causes the layer of deposited particles to become more compact, which can be seen most clearly in the 2D profile plots in Figures 3(a–3c), and is quantified using the standard deviation of deposition depth (σ_d, Figure 3h). Keeping celerity constant and varying filtration coefficient from 0.1 to 0.9/cm decreases σ_d by magnitudes of 1.48, 0.88, 0.47, 0.31, and 0.24 cm for celerities 0.6, 6, 30, 60, and 90 cm/hr, respectively (Figure S1). Increased filtration coefficients shorten the distance within which a particle can be expected to deposit. Therefore, particles deposit within shorter distances and before they travel deep into the bed. This results in a more compact deposition layer.

For all celerities, increasing the filtration coefficient led to an increase and then a slight decrease in the percentage of particles that deposited (Figures 3g and Figure S2 and Data Set S2). The filtration coefficient for which maximal deposition occurred (λ_f^{max}, indicated by black rectangles in Figure S2) was 0.3, 0.4, 0.4, 0.6, and 0.6/cm for celerities 0.6, 6, 30, 60, and 90 cm/hr, respectively. Increases in deposition percentage from $\lambda_f = 0.1$/cm to λ_f^{max} were 14.5%, 16.1%, 18.4%, 20.1%, and 20.0% for the same celerities. Decreases in deposition percentage from λ_f^{max} to $\lambda_f = 0.9$/cm were 6.9%, 6.5%, 3.9%, 3.0%, and 1.5% for the same celerities. Increasing the filtration

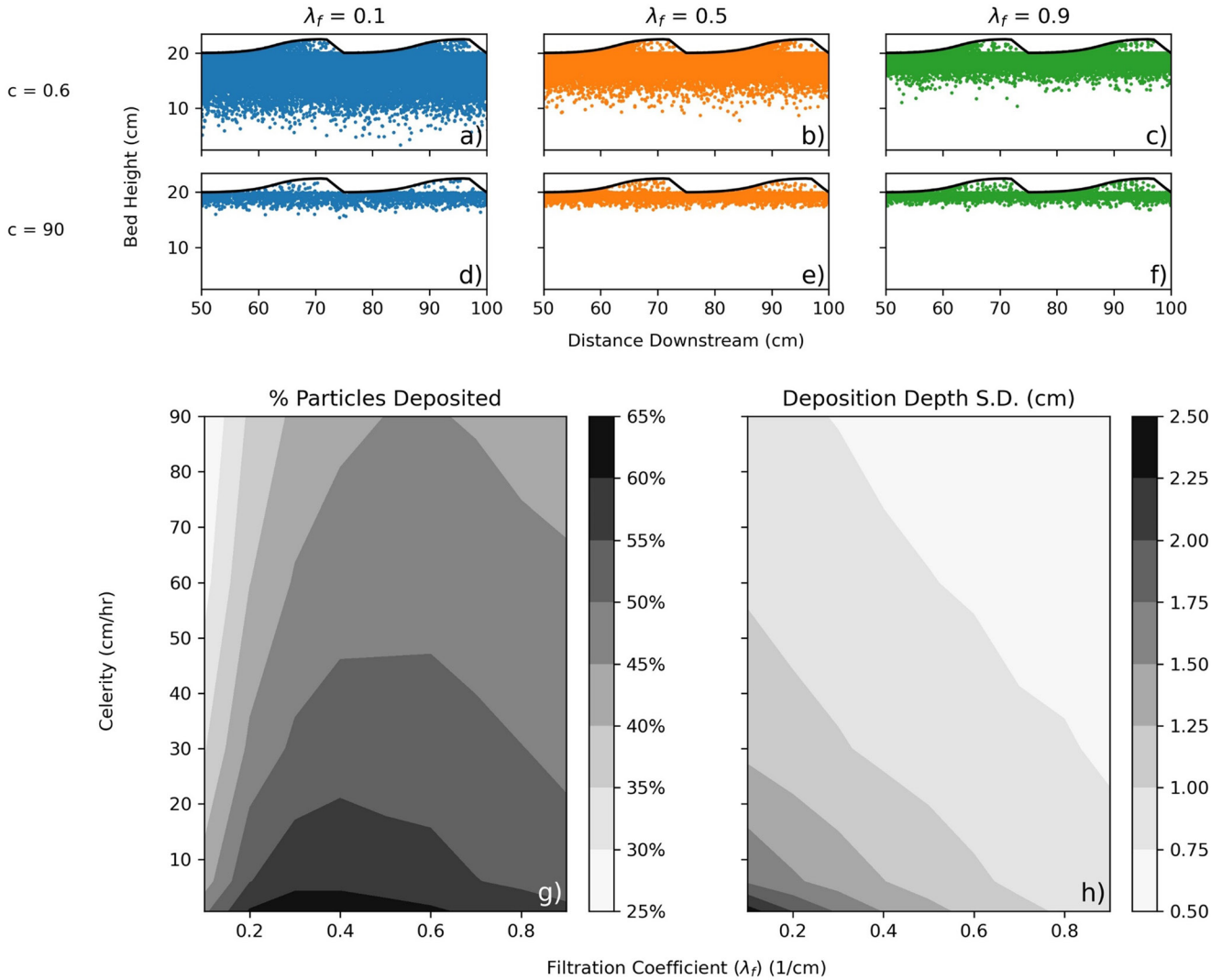

Figure 3. Effects of celerity and filtration coefficient on particle deposition. All panels show results after the passage of five bedforms through the model domain. Panels (a)–(f) show 2D spatial distributions of particles for the slowest and fastest celerities (0.6 and 90 cm/hr). Panels (g) and (h) show phase spaces of filtration coefficient versus celerity in terms of percentage of particles deposited in the bed and standard deviation of deposition depth (σ_d).

coefficient means that the average distance that particles travel before depositing is shorter. The increase for low filtration coefficients ($\lambda_f < \lambda_f^{max}$) occurs because more particles deposit instead of advecting out of the bed. The decrease for higher filtration coefficients ($\lambda_f > \lambda_f^{max}$) is indicative of particles that would otherwise travel below the MFSD instead of depositing above it and later being scoured away.

Increasing celerity also causes the deposition layer to become more compact. σ_d decreases with increasing celerity in all cases (Figures 3h and Figure S3). The decrease in σ_d is greatest for the smallest filtration coefficient (λ_f = 0.1/cm, decrease of 1.52 cm) and conversely the smallest decline in σ_d occurs for the largest filtration coefficient (λ_f = 0.9/cm, decrease of 0.27 cm). Increasing celerity flattens particle flow paths within the bed (Movie S3) restricting particles to a shallower portion of the bed, resulting in a more compact deposition layer (Figures 3a–3f). Flow paths flatten as a result of the migration of the flow field. This occurs due to the faster migration of the upwelling zone relative to the velocities of the particles within the bed, resulting in particles being drawn into an upwelling zone sooner than under stationary bed conditions. Unlike the filtration coefficient, increasing celerity decreased the percentage of particles deposited over the entire range of celerities examined (Figures 3g and Figure S4). The greatest decrease is found for λ_f = 0.1/cm, for which the percentage of particles

released decreases from 49% to 25% between celerities 0.6 and 90 cm/hr. The smallest decrease is for $\lambda_f = 0.9$/cm, for which the decrease is from 56% to 44% between the same celerities.

4. Conclusions

Our results clearly show that there is an interaction between the effects of celerity and filtration coefficient on particle deposition and remobilization. An increase in either bedform celerity or filtration causes particles to deposit at shallower locations (Figures S5–S9). However, an increase in filtration coefficient causes more particles to accumulate in the deposition layer only in some cases, while an increase in celerity results in less accumulation for all cases examined. The decrease in particle accumulation under increased celerity is due to the fact that higher celerity flattens particle flow paths, causing particles to travel less distance in the bed before flowing back out to the water column. Furthermore, the effect of either parameter is modulated by the other. Increasing either parameter causes a more compact deposition layer, but this effect is less prevalent if the other parameter value is high. Similarly, each parameter has a different effect on deposition rate if the other parameter value is high. These findings imply that when studying particle deposition in streams it is important to include measurements of both the bed morphodynamics and interactions between bed sediments and suspended particles (as represented here by the filtration coefficient).

One main consequence of particle deposition in streambeds is clogging due to clay accumulation in the bed (Dallmann et al., 2020; Fox et al., 2014; Shrivastava et al., 2020). The common assumption is that high-flow event and scours prevent clogging from being significant, however, it is clear that the compactness and depth of the clogging layer will affect the scour due to increased cohesion of the bed (Baas et al., 2016; Debnath & Chaudhuri, 2010; Molinas & Hosni, 1999; Wan, 1985). Clogging and reduction in streambed hydraulic conductivity has also been widely observed, but previous studies have not evaluated how the depth of deposition may influence the long-term persistence of the clogging problem (Cheng et al., 2013; Fetzer et al., 2017; Korus et al., 2018, 2020). Depth of deposition is also critical for evaluating the link between streambed morphodynamics and water column turbidity (Bash et al., 2001; Lloyd et al., 1987; Wharton et al., 2017).

Particle deposition also has implications for the health of humans and other organisms. For example, deposited pathogens are released back into the water during bedform scour (Drummond et al., 2017; Rebaudet et al., 2013). Thus, the risk for pathogen resuspension is higher when deposition occurs at shallow depths, as when filtration and celerity increase. Increased depth of deposition means longer residence time in the bed (Harvey et al., 2012; Phillips et al., 2019; Voepel et al., 2013). Longer residence time in turn increases the chances of sediment-dwelling creatures or burrowers ingesting fine particles, such as microplastics, with harmful effects (Garcia et al., 2020; López-Rojo et al., 2020; Wright et al., 2013).

Increased depth of deposition and residence time also have far-reaching implications for microbial respiration and the health of the stream ecosystem. For instance, longer residence time often means enhanced nutrient removal (Briggs et al., 2014; Reeder et al., 2018; Zarnetske et al., 2011). Burial of particulate organic matter has a direct influence on its availability, respiration rates, and metabolic hot spots (Rowland et al., 2017; Stelzer et al., 2014). Enhanced microbial activity and biomass growth may also influence flow paths in the bed due to clogging (Mendoza-Lera & Datry, 2017; Newcomer et al., 2016; Nowinski et al., 2011), and should be taken into account when sampling of sediment is conducted in the field.

The model presented here, adopting a stationary frame of reference, enables the quantification of fine particle accumulation at fixed locations in the bed, within and below the scour zone. The use of a moving boundary to represent the sediment-water interface enables resolving the effects of realistic, time-varying bed morphologies that are commonly found in sand-bed rivers (McElroy & Mohrig, 2009), including the effects of unsteadiness that is commonly found in systems with mixed clay-sand beds (Baas & Best, 2002).

Conflict of Interest

The authors declare no conflicts of interest relevant to this study.

Data Availability Statement

Code and datasets have been uploaded to Hydroshare at https://www.hydroshare.org/resource/90acd3c1c2754e839e1e12d73154eaff/. The Hydroshare repository can be accessed via the following DOI: https://doi.org/10.4211/hs.90acd3c1c2754e839e1e12d73154eaff and can be cited as follows: Teitelbaum et al. (2021). A Novel Framework for Simulating Particle Deposition with Moving Bedforms, HydroShare, http://www.hydroshare.org/resource/90acd3c1c2754e839e1e12d73154eaff.

Acknowledgments
This research was supported by a grant from the U.S.-Israel Binational Science Foundation (BSF), and the U.S. National Science Foundation (NSF; award number EAR-1734300) via the NSF-BSF joint program in Earth Sciences, and by the Israel Science Foundation (Grant No. 647/21 to SA, and 1872/19 to SKH).

References

Arce, G., Montecinos, M., Guerra, P., Escauriaza, C., Coquery, M., & Pastén, P. (2017). Enhancement of particle aggregation in the presence of organic matter during neutralization of acid drainage in a stream confluence and its effect on arsenic immobilization. *Chemosphere*, *180*, 574–583. https://doi.org/10.1016/j.chemosphere.2017.03.107

Baas, J. H., & Best, J. L. (2002). Turbulence modulation in clay-rich sediment-laden flows and some implications for sediment deposition. *Journal of Sedimentary Research*, *72*(3), 336–340. https://doi.org/10.1306/120601720336

Baas, J. H., Best, J. L., & Peakall, J. (2016). Predicting bedforms and primary current stratification in cohesive mixtures of mud and sand. *Journal of the Geological Society*, 12–45. https://doi.org/10.1144/jgs2015-024

Bash, J., Berman, C., & Bolton, S. (2001). *Effects of turbidity and suspended solids on salmonids*.

Briggs, M. A., Lautz, L. K., & Hare, D. K. (2014). Residence time control on hot moments of net nitrate production and uptake in the hyporheic zone. *Hydrological Processes*, *28*(11), 3741–3751. https://doi.org/10.1002/hyp.9921

Brunke, M. (1999). Colmation and depth filtration within streambeds: Retention of particles in hypoheic interstices. *International Review of Hydrobiology*, *84*(2), 99–117. https://doi.org/10.1002/iroh.199900014

Brunke, M., & Gonser, T. (1997). The ecological significance of exchange processes between rivers and groundwater. *Freshwater Biology*, *37*(1), 1–33. https://doi.org/10.1046/j.1365-2427.1997.00143.x

Boano, F., Harvey, J. W., Marion, A., Packman, A. I., Revelli, R., Ridolfi, L., & Wörman, A. (2014). Hyporheic flow and transport processes: Mechanisms, models, and biogeochemical implications. *Reviews of Geophysics*, *52*(4), 603–679. https://doi.org/10.1002/2012RG000417

Cheng, D. H., Chen, X. H., Huo, A. D., Gao, M., & Wang, W. K. (2013). Influence of bedding orientation on the anisotropy of hydraulic conductivity in a well-sorted fluvial sediment. *International Journal of Sediment Research*, *28*(1), 118–125. https://doi.org/10.1016/S1001-6279(13)60024-4

Dallmann, J., Phillips, C. B., Teitelbaum, Y., Sund, N., Schumer, R., Arnon, S., & Packman, A. I. (2020). Impacts of suspended clay particle deposition on sand-bed morphodynamics. *Water Resources Research*, *56*(8), e2019WR027010. https://doi.org/10.1029/2019WR027010

Debnath, K., & Chaudhuri, S. (2010). Laboratory experiments on local scour around cylinder for clay and clay-sand mixed beds. *Engineering Geology*, *111*(1–4), 51–61. https://doi.org/10.1016/j.enggeo.2009.12.003

Droppo, I. G., D'Andrea, L., Krishnappan, B. G., Jaskot, C., Trapp, B., Basuvaraj, M., & Liss, S. N. (2014). Fine-sediment dynamics: Towards an improved understanding of sediment erosion and transport. *Journal of Soils and Sediments*, *15*(2), 467–479. https://doi.org/10.1007/s11368-014-1004-3

Drummond, J., Larsen, L. G., Gonzalez-Pinzon, R., Packman, A. I., & Harvey, J. W. (2017). Fine particle retention within stream storage areas at base flow and in response to a storm event. *Water Resources Research*, *53*(7), 5690–5705. https://doi.org/10.1111/j.1752-1688.1969.tb04897.x

Drummond, J., Schmadel, N., Kelleher, C., Packman, A., & Ward, A. (2019). Improving predictions of fine particle immobilization in streams. *Geophysical Research Letters*, *46*(23), 13853–13861. https://doi.org/10.1029/2019GL085849

Einstein, H. A. (1950). The bed-load function for sediment transportation in open channel flows. Technical Bulletin 156389, *United States Department of Agriculture, Economic Research Service*.

Elliott, H., & Brooks, N. H. (1997). Transfer of nonsorbing solutes to a streambed with bed forms: Theory. *Water Resources Research*, *33*(1), 123–136. https://doi.org/10.1029/96WR02784

Engelund, F., & Hansen, E. (1967). *A monograph on sediment transport in alluvial streams*.

Fetzer, J., Holzner, M., Plotze, M., & Furrer, G. (2017). Clogging of an alpine streambed by silt-sized particles- Insights from laboratory and field experiments. *Water Research*, *126*, 60–69. https://doi.org/10.1016/j.watres.2017.09.015

Foster, I. D. L., & Charlesworth, S. M. (1996). Heavy metals in the hydrological cycle: Trends and explanation. *Hydrological Processes*, *10*(2), 227–261. https://doi.org/10.1002/(SICI)1099-1085(199602)10:2<227::AID-HYP357>3.0.CO;2-X

Fox, A., Packman, A. I., Boano, F., Phillips, C. B., & Arnon, S. (2018). Interactions between suspended kaolinite deposition and hyporheic exchange flux under losing and gaining flow conditions. *Geophysical Research Letters*, *45*(9), 4077–4085. https://doi.org/10.1029/2018GL077951

Garcia, T. D., Cardozo, A. L. P., Quirino, B. A., Yofukuji, K. Y., Ganassin, M. J. M., dos Santos, N. C. L., & Fugi, R. (2020). Ingestion of microplastic by fish of different feeding habits in urbanized and non-urbanized streams in southern Brazil. *Water, Air, and Soil Pollution*, *231*(8), 434. https://doi.org/10.1007/s11270-020-04802-9

Harris, C. R., Millman, K. J., van der Walt, S. J., Gommers, R., Virtanen, P., Cournapeau, D., et al. (2020). Array programming with NumPy. *Nature*, *585*, 357–362. https://doi.org/10.1038/s41586-020-2649-2

Harvey, J. W., Drummond, J. D., Martin, R. L., McPhillips, L. E., Packman, A. I., Jerolmack, D. J., et al. (2012). Hydrogeomorphology of the hyporheic zone: Stream solute and fine particle interactions with a dynamic streambed. *Journal of Geophysical Research: Biogeosciences*, *117*(4), 1–20. https://doi.org/10.1029/2012JG002043

Hope, D., Billett, M. F., & Cresser, M. S. (1994). A review of the export of carbon in river water: Fluxes and processes. *Environmental Pollution*, *84*(3), 301–324. https://doi.org/10.1016/0269-7491(94)90142-2

Hunter, J. D. (2007). Matplotlib: A 2D graphics environment. *Computing in Science & Engineering*, *9*(3), 90–95. https://doi.org/10.1109/MCSE.2007.55

Jin, G., Zhang, Z., & Barry, D. A. (2019). Colloid transport and distribution in the hyporheic zone. *Hydrological Processes*, *33*, 932–944. https://doi.org/10.1002/hyp.13375

Johnson, E. R., Inamdar, S., Kan, J., & Vargas, R. (2018). Particulate organic matter composition in stream runoff following large storms: Role of POM sources, particle size, and event characteristics. *Journal of Geophysical Research: Biogeosciences*, *123*(2), 660–675. https://doi.org/10.1002/2017JG004249

Kessler, A. J., Cardenas, M. B., & Cook, P. L. M. (2015). The negligible effect of bed form migration on denitrification in hyporheic zones of permeable sediments, *120*(3), 1–11. https://doi.org/10.1002/2014JG002852

Korus, J. T., Fraundorfer, W. P., Gilmore, T. E., & Karnik, K. (2020). Transient streambed hydraulic conductivity in channel and bar environments, Loup River, Nebraska. *Hydrological Processes*, *26*, 3061–3077. https://doi.org/10.1002/hyp.13777

Korus, J. T., Gilmore, T. E., Waszgis, M. M., & Mittelstet, A. R. (2018). Unit-bar migration and bar-trough deposition: Impacts on hydraulic conductivity and grain size heterogeneity in a sandy streambed. *Hydrogeology Journal*, *26*(2), 553–564. https://doi.org/10.1007/s10040-017-1661-6

Lenaker, P. L., Corsi, S. R., McLellan, S. L., Borchardt, M. A., Olds, H. T., Dila, D. K., et al. (2018). Human-associated indicator bacteria and human-specific viruses in surface water: A spatial assessment with implications on fate and transport. *Environmental Science and Technology*, *52*(21), 12162–12171. https://doi.org/10.1021/acs.est.8b03481

Li, C., Busquets, R., & Campos, L. C. (2020). Assessment of microplastics in freshwater systems: A review. The *Science of the Total Environment*, *707*, 135578. https://doi.org/10.1016/j.scitotenv.2019.135578

Lloyd, D. S., Koenings, J. P., & Laperriere, J. D. (1987). Effects of turbidity in fresh waters of Alaska. *North American Journal of Fisheries Management*, *7*(1), 18–33.

López-Rojo, N., Pérez, J., Alonso, A., Correa-Araneda, F., & Boyero, L. (2020). Microplastics have lethal and sublethal effects on stream invertebrates and affect stream ecosystem functioning. *Environmental Pollution*, *259*, 113898. https://doi.org/10.1016/j.envpol.2019.113898

McElroy, B., & Mohrig, D. (2009). Nature of deformation of sandy bed forms. *Journal of Geophysical Research: Solid Earth*, *114*, F00A04. https://doi.org/10.1029/2008JF001220

McKinney, W. (2010). Data structures for statistical computing in Python. In *Proceedings of the 9th Python in Science Conference* (pp. 56–61). https://doi.org/10.25080/majora-92bf1922-00a

Mendoza-Lera, C., & Datry, T. (2017). Relating hydraulic conductivity and hyporheic zone biogeochemical processing to conserve and restore river ecosystem services. The *Science of the Total Environment*, *579*, 1815–1821. https://doi.org/10.1016/j.scitotenv.2016.11.166

Molinas, A., & Hosni, M. M. (1999). Effects of gradation and cohesion on bridge scour: Volume 4: Experimental study of scour around circular piers in cohesive Soils(Vol. *4*), *US Department of Transportation, Federal Highway Administration*.

Newbold, J. D., Thomas, S. A., Minshall, G. W., Cushing, C. E., & Georgian, T. (2005). Deposition, benthic residence, and resuspension of fine organic particles in a mountain stream. *Limnology & Oceanography*, *50*(5), 1571–1580.

Newcomer, M. E., Hubbard, S. S., Fleckenstein, J. H., Maier, U., Schmidt, C., Thullner, M., et al. (2016). Simulating bioclogging effects on dynamic riverbed permeability and infiltration. *Water Resources Research*, *52*(4), 2883–2900. https://doi.org/10.1111/j.1752-1688.1969.tb04897.x

Nowinski, J. D., Cardenas, M. B., & Lightbody, A. F. (2011). Evolution of hydraulic conductivity in the floodplain of a meandering river due to hyporheic transport of fine materials. *Geophysical Research Letters*, *38*(1), 2–6. https://doi.org/10.1029/2010GL045819

Packman, A. I., & Brooks, N. H. (2001). Hyporheic exchange of solutes and colloids with moving bed forms. *Water Resources Research*, *37*(10), 2591–2605. https://doi.org/10.1029/2001WR000477

Packman, A. I., Brooks, N. H., & Morgan, J. J. (2000a). A physicochemical model for colloid exchange between a stream and a sand streambed with bed forms. *Water Resources Research*, *36*(8), 2351–2361. https://doi.org/10.1029/2000WR900059

Packman, A. I., Brooks, N. H., & Morgan, J. J. (2000b). Kaolinite exchange between a stream and streambed: Laboratory experiments and validation of a colloid transport model. *Water Resources Research*, *36*(8), 2363–2372. https://doi.org/10.1029/2000WR900058

Packman, A. I., & Mackay, J. S. (2003). Interplay of stream-subsurface exchange, clay particle deposition, and streambed evolution. *Water Resources Research*, *39*(4), 1–10. https://doi.org/10.1029/2002WR001432

Park, J., & Hunt, J. R. (2018). Modeling fine particle dynamics in gravel-bedded streams: Storage and re-suspension of fine particles. The *Science of the Total Environment*, *634*, 1042–1053. https://doi.org/10.1016/j.scitotenv.2018.04.034

Partington, D., Therrien, R., Simmons, C. T., & Brunner, P. (2017). Blueprint for a coupled model of sedimentology, hydrology, and hydrogeology in streambeds. *Reviews of Geophysics*, *55*(2), 287–309. https://doi.org/10.1002/2016RG000530

Phillips, C. B., Dallmann, J. D., Jerolmack, D. J., & Packman, A. I. (2019). Fine-particle deposition, retention, and resuspension within a sand-bedded stream are determined by streambed morphodynamics. *Water Resources Research*, *55*(12), 303–318. https://doi.org/10.1029/2019WR025272

Preziosi-Ribero, A., Packman, A. I., Escobar-Vargas, J. A., Phillips, C. B., Donado, L. D., & Arnon, S. (2020). Fine sediment deposition and filtration under losing and gaining flow conditions: A particle tracking model approach. *Water Resources Research*, *56*(2), 1–14. https://doi.org/10.1029/2019WR026057

Rebaudet, S., Gazin, P., Barrais, R., Moore, S., Rossignol, E., Barthelemy, N., et al. (2013). The dry season in Haiti: A window of opportunity to eliminate cholera. *PLoS Currents*, *5*(Outbreaks). https://doi.org/10.1371/currents.outbreaks.2193a0ec4401d9526203af12e5024ddc

Reeder, W. J., Quick, A. M., Farrell, T. B., Benner, S. G., Feris, K. P., Marzadri, A., & Tonina, D. (2018). Hyporheic source and sink of nitrous oxide. *Water Resources Research*, *54*(7), 5001–5016. https://doi.org/10.1029/2018WR022564

Rehg, K. J., Packman, A. I., & Ren, J. (2005). Effects of suspended sediment characteristics and bed sediment transport on streambed clogging. *Hydrological Processes*, *19*(2), 413–427. https://doi.org/10.1002/hyp.5540

Rowland, R., Inamdar, S., & Parr, T. (2017). Evolution of particulate organic matter (POM) along a headwater drainage: Role of sources, particle size class, and storm magnitude. *Biogeochemistry*, *133*(2), 181–200. https://doi.org/10.1007/s10533-017-0325-x

Shrivastava, S., Stewardson, M. J., & Arora, M. (2020). Distribution of clay-sized sediments in streambeds and influence of fine sediment clogging on hyporheic exchange. *Hydrological Processes*, *34*(26), 5674–5685. https://doi.org/10.1002/hyp.13988

Stelzer, R. S., Thad Scott, J., Bartsch, L. A., & Parr, T. B. (2014). Particulate organic matter quality influences nitrate retention and denitrification in stream sediments: Evidence from a carbon burial experiment. *Biogeochemistry*, *119*(1–3), 387–402. https://doi.org/10.1007/s10533-014-9975-0

Stone, M., & Droppo, I. G. (1994). In-channel surficial fine-grained sediment laminae. Part II: Chemical characteristics and implications for contaminant transport in fluvial systems. *Hydrological Processes*, *8*(2), 113–124.

Teitelbaum, Y., Dallmann, J., Phillips, C. B., Packman, A. I., Schumer, R., Sund, N. L., et al. (2021). Dynamics of hyporheic exchange flux and fine particle deposition under moving bedforms. *Water Resources Research*, *57*(4), 1–13. https://doi.org/10.1029/2020wr028541

van Rijn, L. (1993). *Principles of sediment transport in rivers, Estuaries and Coastal Seas. Principles of sediment transport in rivers, Estuaries and Coastal Seas*. Aqua Publications.

Virtanen, P., Gommers, R., Oliphant, T. E., Haberland, M., Reddy, T., Cournapeau, D., et al. (2020). SciPy 1.0: Fundamental algorithms for scientific computing in Python. *Nature Methods*, *17*(3), 261–272. https://doi.org/10.1038/s41592-019-0686-2

Voepel, H., Schumer, R., & Hassan, M. A. (2013). Sediment residence time distributions: Theory and applications from bed elevation measurements. *JGR Earth Surface*, *118*(4), 2557–2567. https://doi.org/10.1002/jgrf.20151

Wan, Z. (1985). Bed material movement in hyperconcentrated flow. *Journal of Hydraulic Engineering*, *111*(6), 987–1002.

Wharton, G., Mohajeri, S. H., & Righetti, M. (2017). The pernicious problem of streambed colmation: A multi-disciplinary reflection on the mechanisms, causes, impacts, and management challenges. *WIREs Water*, *4*, e1231. https://doi.org/10.1002/wat2.1231

Wolke, P., Teitelbaum, Y., Deng, C., Lewandowski, J., & Arnon, S. (2020). Impact of bed form celerity on oxygen dynamics in the hyporheic zone. *Water*, *12*(1), 5–7. https://doi.org/10.3390/w12010062

Wright, S. L., Thompson, R. C., & Galloway, T. S. (2013). The physical impacts of microplastics on marine organisms: A review. *Environmental Pollution*, *178*, 483–492. https://doi.org/10.1016/j.envpol.2013.02.031

Zarnetske, J. P., Haggerty, R., Wondzell, S. M., & Baker, M. A. (2011). Dynamics of nitrate production and removal as a function of residence time in the hyporheic zone. *Journal of Geophysical Research: Biogeosciences*, *116*, G01025. https://doi.org/10.1029/2010JG001356

Zheng, L., Cardenas, M. B., Wang, L., & Mohrig, D. (2019). Ripple effects: Bed form morphodynamics cascading into hyporheic zone biogeochemistry. *Water Resources Research*, *55*(8), 7320–7342. https://doi.org/10.1029/2018wr023517

References From the Supporting Information

Ahmerkamp, S., Winter, C., Janssen, F., Kuypers, M. M. M., & Holtappels, M. (2015). The impact of bedform migration on benthic oxygen fluxes. *Journal of Geophysical Research: Biogeosciences*, 1–14. https://doi.org/10.1002/2015JG003106

Arcement, G. J., & Schneider, V. R. (1989). Guide for selecting Manning's roughness coefficients for natural channels and flood plains. *United States Geological Survey*. Water Supply paper 2339, Denver.

Arnon, S., Marx, L. P., Searcy, K. E., & Packman, A. I. (2010). Effects of overlying velocity, particle size, and biofilm growth on stream-subsurface exchange of particles. *Hydrological Processes*, *114*, 108–114. https://doi.org/10.1002/hyp

Dey, S. (2014). *Fluvial Hydrodynamics*. Springer-Verlag. https://doi.org/10.1007/978-3-642-19062-9

Elliott, H., & Brooks, N. H. (1997). Transfer of nonsorbing solutes to a streambed with bed forms: Theory . *Water Resources Research*, *33*(1), 123–136. https://doi.org/10.1029/96WR02784

Fehlman, H. M. (1985). Resistance components and velocity distributions of open channel flows over bedforms. *Geological Survey Water Supply 1592*, US Geological Survey.

Fox, A., Boano, F., & Arnon, S. (2014). Impact of losing and gaining streamflow conditions on hyporheic exchange fluxes induced by dune-shaped bed forms. *Water Resources Research*, *50*(3), 1895–1907. https://doi.org/10.1002/2013WR014333

Janssen, F., Cardenas, M. B., Sawyer, A. H., Dammrich, T., Krietsch, J., & De Beer, D. (2012). A comparative experimental and multiphysics computational fluid dynamics study of coupled surface-subsurface flow in bed forms. *Water Resources Research*, *48*(8), 1–16. https://doi.org/10.1029/2012WR011982

Karim, F. (1995). Bed configuration and hydraulic resistance in alluvial-channel flows. *Journal of Hydraulic Engineering*, *121*(1), 15–25.

Lichtman, I. D., Baas, J. H., Amoudry, L. O., Thorne, P. D., Malarkey, J., Hope, J. A., et al. (2018). Bedform migration in a mixed sand and cohesive clay intertidal environment and implications for bed material transport predictions. *Geomorphology*, *315*, 17–32. https://doi.org/10.1016/j.geomorph.2018.04.016

Packman, A. I., & Brooks, N. H. (2001). Hyporheic exchange of solutes and colloids with moving bed forms. *Water Resources Research*, *37*(10), 2591–2605. https://doi.org/10.1029/2001WR000477

Packman, A. I., Brooks, N. H., & Morgan, J. J. (2000). Kaolinite exchange between a stream and streambed: Laboratory experiments and validation of a colloid transport model. *Water Resources Research*, *36*(8), 2363–2372. https://doi.org/10.1029/2000WR900058

Raudkivi, A. J. (1997). Ripples on stream bed. *Journal of Hydraulic Engineering*, *123*(1), 58–64.

Snishchenko, B. F., & Kopaliani, Z. D. (1978). On the bedforms velocity in rivers and flumes (in Russian). *Proceedings of the. State Hydr. Inst.*, *252*, 30–37.

Soulsby, R. L., Whitehouse, R. J. S., & Marten, K. V. (2012). Prediction of time-evolving sand ripples in shelf seas. *Continental Shelf Research*, *38*, 47–62. https://doi.org/10.1016/j.csr.2012.02.016

Teitelbaum, Y., Dallmann, J., Phillips, C. B., Packman, A. I., Schumer, R., Sund, N. L., et al. (2021). Dynamics of hyporheic exchange flux and fine particle deposition under moving bedforms. *Water Resources Research*, *57*(4), 1–13. https://doi.org/10.1029/2020wr028541

Toride, N., Leij, F. J., & Van Genuchten, M. T. (1995). *The CXTFIT code for estimating transport parameters from laboratory or field tracer experiments*. Retrieved from http://www.researchgate.net/publication/247824027_The_CXTFIT_Ver_2.0._Code_for_estimating_transport_parameters_from_laboratory_or_field_tracer_experiments

van Rijn, L. (1993). *Principles of sediment transport in rivers, Estuaries and Coastal Seas. Principles of sediment transport in rivers, Estuaries and Coastal Seas*. Aqua Publications.

Wolke, P., Teitelbaum, Y., Deng, C., Lewandowski, J., & Arnon, S. (2020). Impact of bed form celerity on oxygen dynamics in the hyporheic zone. *Water*, *12*(1), 5–7. https://doi.org/10.3390/w12010062

Zheng, L., Cardenas, M. B., Wang, L., & Mohrig, D. (2019). Ripple effects: Bed form morphodynamics cascading into hyporheic zone biogeochemistry. *Water Resources Research*, *55*(8), 7320–7342. https://doi.org/10.1029/2018wr023517